JOM, Vol. 69, No. 2, 2017
DOI: 10.1007/s11837-016-2200-y

The Influence of Heat Treatment on the Optical Parameters of Spray-Deposited CdS: In Thin Films

SHADIA J. IKHMAYIES[1,2]

1.—Faculty of Science, Physics Department, Al Isra University, Amman 11622, Jordan.
2.—e-mail: shadia_ikhmayies@yahoo.com

Cadmium sulfide is an important material for solar cells and optoelectronic devices. For the development of these technologies, a comprehensive optical characterization of this material is required. Doping with indium affects the optical parameters of CdS. In this study, indium-doped cadmium sulfide thin films (CdS:In) were produced by the spray pyrolysis technique. The films were annealed in a nitrogen atmosphere, and the influence of annealing on the optical parameters was investigated. Transmittance was measured and used to deduce absorption coefficient, bandgap energy, extinction coefficient, refractive index, real and imaginary parts of the dielectric constant, optical conductivity, and energy loss before and after annealing. Tailing in the bandgap was assumed to follow Urbach tailing, and the effect of annealing on the width of the tail was studied. Dispersion of the refractive index was analyzed using the single oscillator model, and the influence of annealing on the dispersion parameters is discussed.

INTRODUCTION

Cadmium sulfide (CdS) is a II–VI compound semiconductor of a wide bandgap of about 2.42 eV at room temperature. CdS has reasonable conversion efficiency, stability and mature low-cost deposition technique. In addition, it has high electron affinity and it is easy to make ohmic contact. CdS thin films have potential uses in optoelectronic device fabrication and in photovoltaic applications as a window layer in CdTe-based and $CuInS_2$ solar cells. For use as window layers in thin-film solar cells, CdS must have *n*-type electrical conductivity. There are different dopants that can be used to obtain *n*-type CdS, such as In Refs. 1–4, Ag,[1] Al,[1,5] Cl,[6] etc. In this work, indium was used as the dopant to improve the *n*-type conductivity of CdS films.

There are different techniques to produce CdS thin films such as chemical bath deposition (CBD),[1,7–9] thermal evaporation,[10] and the spray pyrolysis (SP) technique.[11,12] The SP technique is a simple and low-cost method, which enables intentional doping, and the production of large-area films. The study of the optical properties and optimizing the optical parameters of CdS is important for the use of this material in solar cells and optoelectronic devices. The aim of the present work is to pay more attention to studying the influence of annealing on the optical parameters of indium-doped cadmium sulfide (CdS:In) thin films prepared by the spray pyrolysis technique.

EXPERIMENTAL PROCEDURE

Indium-doped cadmium sulfide (CdS:In) thin films were prepared by spraying an aqueous solution of approximately stoichiometric ratios of the hydrated cadmium chloride ($CdCl_2{\cdot}H_2O$) and thiourea [$(NH_2)_2CS$] on glass substrates kept at 490°C. Indium chloride ($InCl_3$) was used as a dopant source in the starting solution. The films thus produced were annealed in a nitrogen atmosphere for 30 min at 400°C. Transmission spectra of the prepared films were measured at room temperature by normal incidence of light, using a double-beam UV-1601 PC Shimadzu spectrophotometer, in the wavelength range 400–1100 nm. The structure of the films was explored using x-ray diffraction (XRD) with CuK_α radiation (λ = 1.5405 Å) in the range of Bragg angles $2° \le 2\theta \le 60°$ in steps of 0.04°. The morphology and composition of the films were investigated using FEI scanning electron microscope (Inspect F 50) equipped with a thin-window

(Published online November 21, 2016)

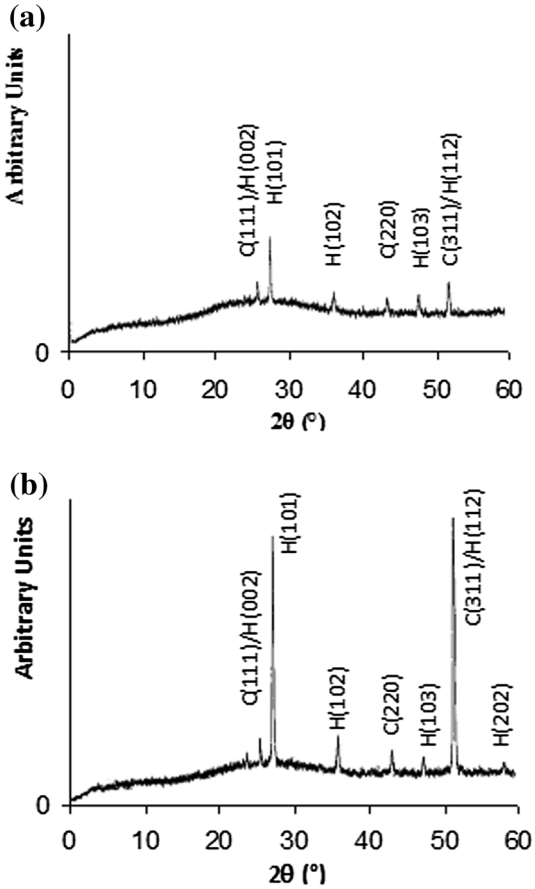

Fig. 1. XRD diffractograms of two CdS:In thin films; as-deposited with thickness = 400 nm (a), and annealed with thickness = 230 nm (b).

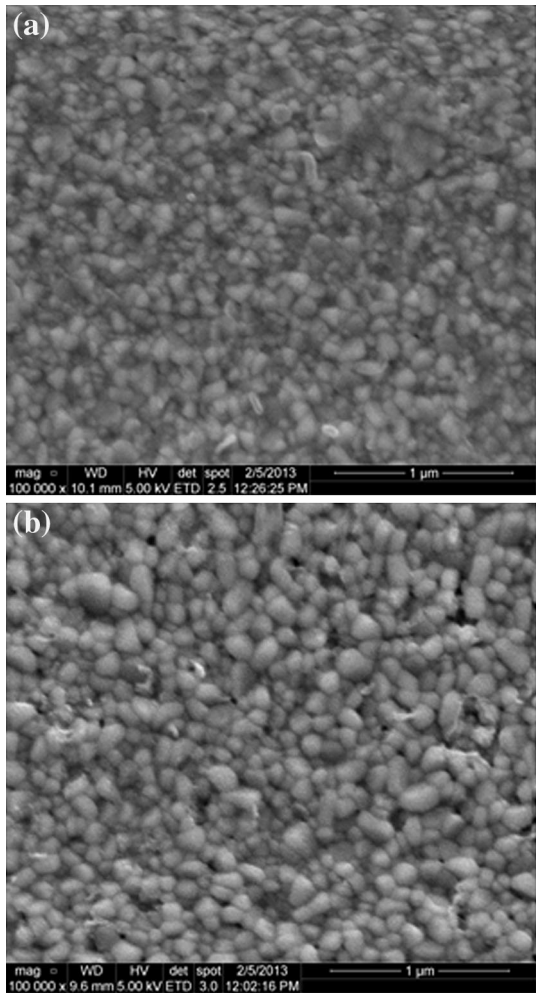

Fig. 2. SEM micrographs of two CdS:In thin films of thickness about 140 nm: as-deposited (a), and annealed (b).

energy dispersive x-ray spectrometer (EDS). The films' thickness was estimated using transmittance and Lambert's law of absorption in a semiconductor.

RESULTS AND DISCUSSION

XRD diffractograms of as-deposited and annealed CdS:In thin films are shown in Fig. 1. The figure reveals that the films are polycrystalline and they have a mixed phase (cubic and hexagonal). All the prominent peaks are indexed with Millar indices which are shown in the figure. The lines C(1 1 1), C(2 2 0), and C(3 1 1) belong to the cubic phase. However, the peaks H(0 0 2), H(1 0 1), H(1 0 2), H(1 0 3), H(1 1 2), and H(2 0 2) belong to the hexagonal phase. The as-deposited and annealed CdS:In films were preferentially oriented along the H(1 0 1), and the C(3 1 1)/H(1 1 2) planes, where the positions of the C(3 1 1) line of the cubic phase and that of the H(1 1 2) line of the hexagonal phase approximately coincide.

SEM micrographs of an as-grown and nitrogen annealed CdS:In thin films on glass substrates are shown in Fig. 2. The films are polycrystalline and the annealed film shows larger grains as can be seen in the Figure. The surfaces of the films appear compact and with good substrate coverage. There is no notable change in surface morphologies between the as-deposited and annealed films. This is because the films were deposited at a high temperature (490°C), so the crystal growth is complete. Figure 3 displays the EDS spectra for the as-deposited (Fig. 3a) and annealed (Fig. 3b) films. From these, it can be seen that the films contain cadmium, sulfur, and indium.

Figure 4 displays the transmittance of films of different thicknesses which are annealed in a nitrogen atmosphere at 400°C. The transmittance decreased with the annealing, and the absorption edge was shifted towards the longer wavelengths, which refers to the decrease in the optical bandgap energy. The decrease in transmittance is related to the improvement in crystallinity and the increase of the number of free charge carriers after annealing.

Absorption coefficient values of the films were deduced from the transmittance data, and they are of the order of 10^4 cm^{-1} in the strong absorption region. Figure 5 depicts the relationship between the absorption coefficient α and the photon's energy

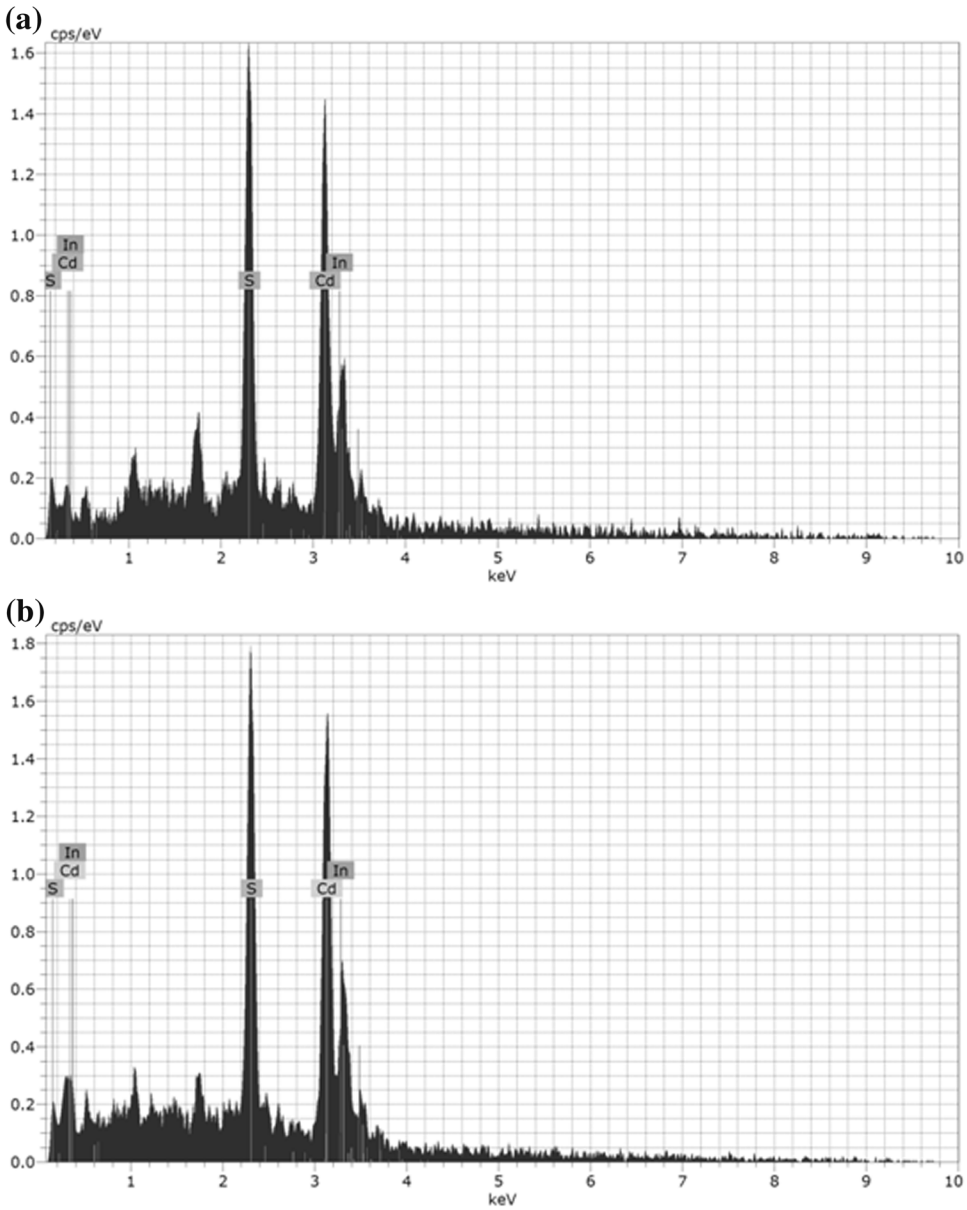

Fig. 3. The EDS plots for the as-deposited (a), and annealed (b) CdS:In thin films of SEM images shown in Fig. 2.

$h\nu$ for CdS:In thin films before and after annealing. From the Figure, it is apparent that the absorption edge was shifted to the lower energy side after annealing. The absorption coefficient increased or stayed approximately constant after annealing in the region of weak absorption, while it increased in the strong absorption region for two films (a and c), decreased for two films (b and d), and stayed approximately constant for another film (e). The decrease of α after annealing may be related to the Cd:S ratios and the indium content in these films. It can noted that the film in (b) and the films in (d and e) have higher transmittance before and after annealing than the films in (a and c). This means that the films in (b, d, and e) have approximately the same or smaller number of free charge carriers after annealing.

To estimate the value of the bandgap energy, a plots of $(\alpha h\nu)^2$ versus $h\nu$ is displayed in Fig. 6, where the transition is assumed to be a direct one. Linear fits were made in the linear regions of the curves, and the optical bandgap energy E_g was estimated from the intercepts with the energy axis. The obtained values of E_g are shown in Fig. 6, and they are in the ranges 2.440–2.448 eV, and 2.414–2.443 eV before and after annealing, respectively. Thus, the annealed films have reduced bandgap values compared with the as-deposited ones.

The absorption coefficient, α, near the fundamental absorption edge usually shows simple exponential energy dependence:[13]

$$\alpha = \alpha_0 \exp(h\nu/E_e) \quad (1)$$

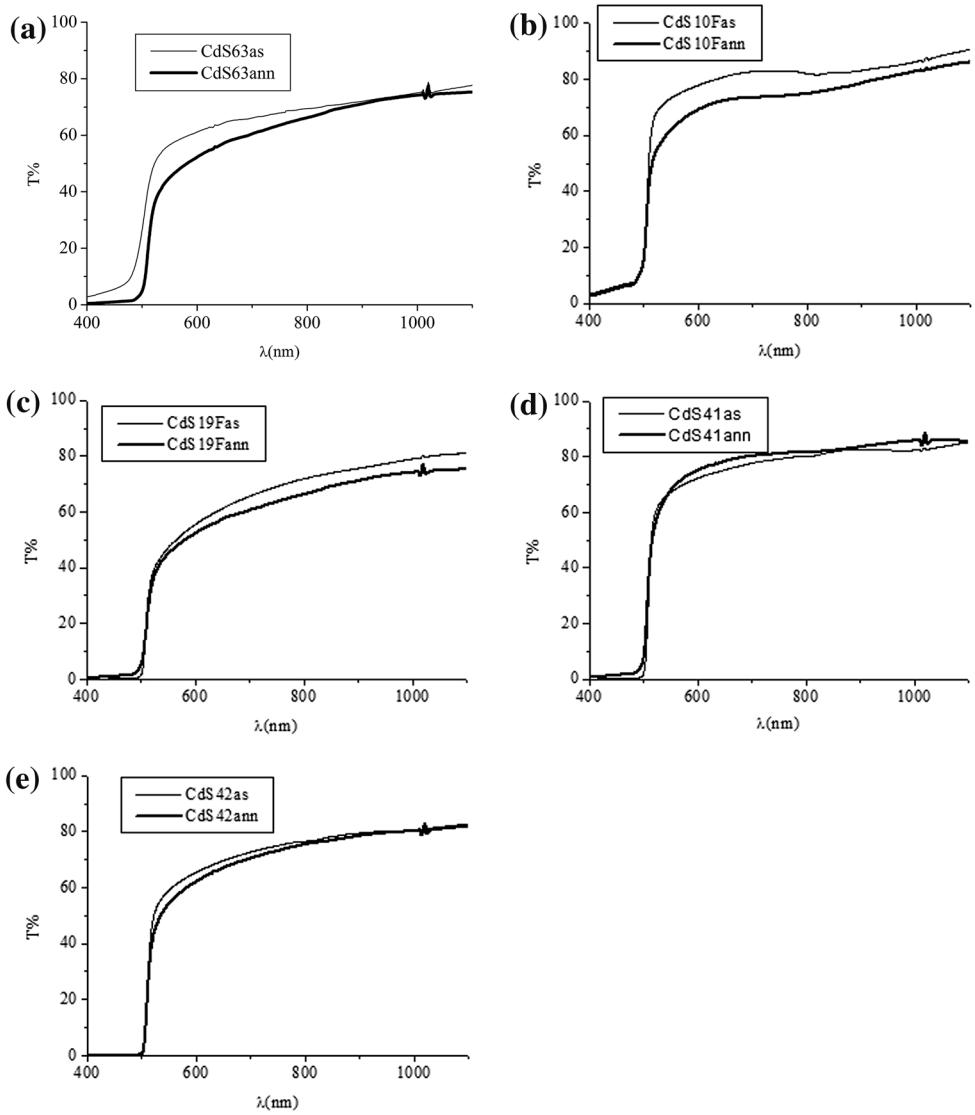

Fig. 4. Transmittance spectra of as-deposited and annealed CdS:In thin films with different thickness *t*. (a) $t = 335$ nm. (b) $t = 400$ nm. (c) $t = 730$ nm. (d) $t = 740$ nm. (e) $t = 800$ nm. The legend contains the names of the samples, where as refers to the as-deposited, and ann to the annealed films.

referred to as the Urbach tail, where α_0 is constant and E_e determines the width of the tail. The tail, i.e., Urbach energy, is generally attributed to disorder in the material which leads to a tail in the valence and conduction bands. To find the value of E_e, a plot of the natural logarithm of the absorption coefficient ($\ln \alpha$) against the photons energy $h\nu$ was made and is shown in Fig. 7. Linear fits were performed in the linear parts of the curves; fit parameters were used to find E_e and α_0. The values are inserted in Table I. In general, it can be noticed that E_e decreases with annealing. The decrease of Urbach energy with annealing could be due to a decrease of the defects density in the tail after heat treatment. The enlargement of grain size results in a narrowing of the grain boundaries and then a reduction in the defects density.

To find the refractive index and the extinction coefficient, the definition of the reflectance R of a film for a light wave incident normally from air, with refractive index $n_0 = 1$, on a medium of complex refractive index $n^* = n + ik$ is used.[14]

$$R = \frac{(n^* - 1)^2}{(n^* + 1)^2} = \frac{(n-1)^2 + k^2}{(n+1)^2 + k^2} \qquad (2)$$

where n is the refractive index and k is the extinction coefficient of the film. Figure 8 shows that the reflectivity R of the films against the photon's energy $h\nu$ for the whole set of films under study. As the figure shows, R increases with annealing, especially in the near-infrared and visible regions. This result is in good agreement with Ziabari and Ghodsi[13] for CdS nanoscrystalline thin films prepared by sol–gel and incorporated in polyethyleneglycol.

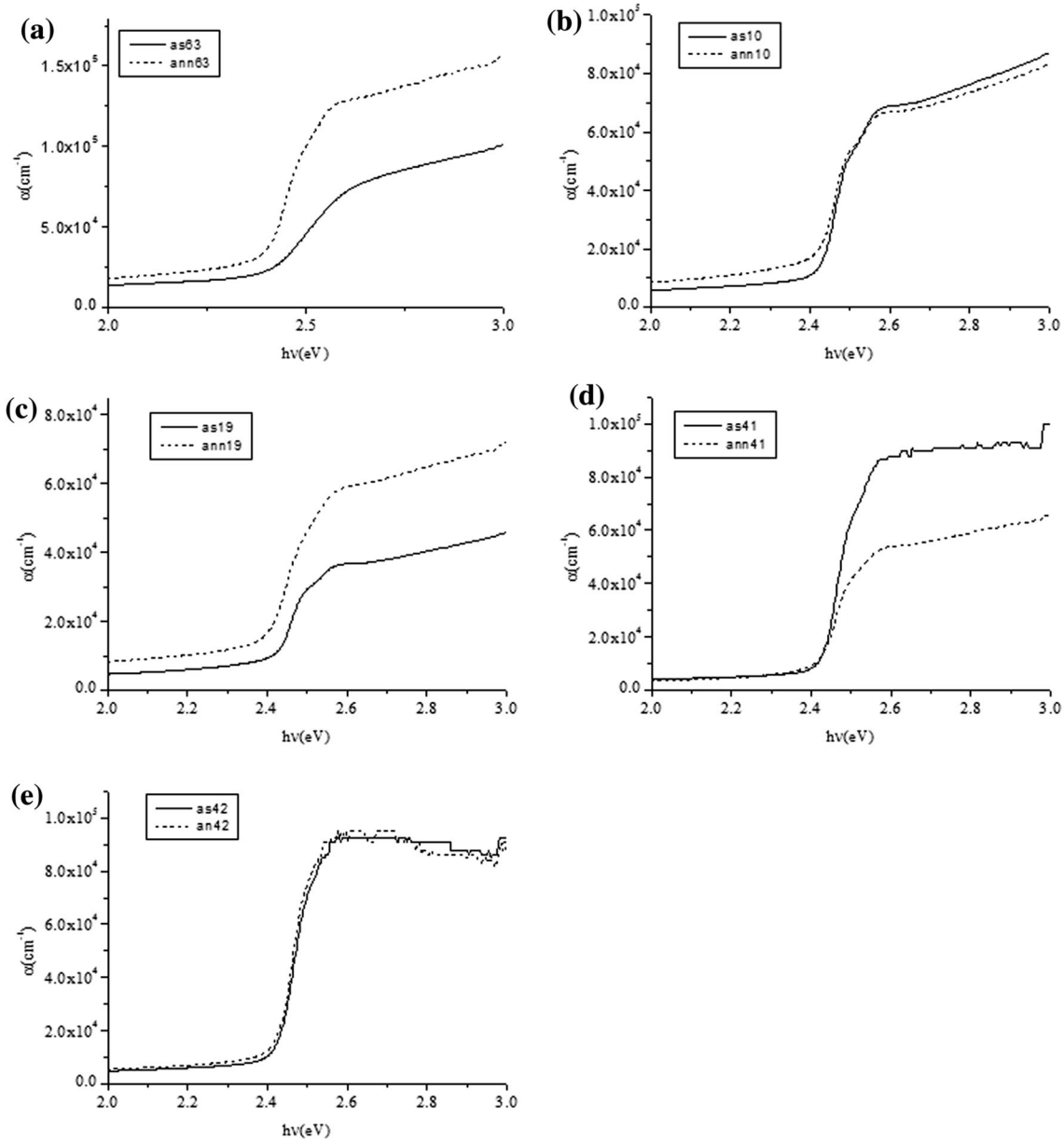

Fig. 5. Absorption coefficient of as-deposited and annealed CdS:In films as a function of the photon's energy $h\nu$ for films with different thickness. (a) t = 336 nm. (b) t = 401 nm. (c) t = 732 nm. (d) t = 741 nm. (e) t = 801 nm.

Knowing the value of the absorption coefficient α from the transmittance, the extinction coefficient can be calculated using the relationship $k = \frac{\lambda\alpha}{4\pi}$, where λ is the wavelength in free space. Solving Eq. 1 for the refractive index n gives;

$$n = \frac{(1+R) + \left[(1+R)^2 - (1-R)^2\left(1+k^2\right)\right]^{1/2}}{1-R} \quad (3)$$

Figure 9 shows the dependence of the extinction coefficient of the films on $h\nu$. It is restricted for all the films in the ranges 0.018–0.077 and 0.019–0.110 before and after annealing, respectively. It is also fairly constant in the regions before the absorption edge. A sharp increase of k occurs at the absorption edge, then it becomes approximately constant or decreases slowly with $h\nu$.

Refractive index n values for all films were calculated using Eq. 3 and plotted against the photon's energy $h\nu$ in Fig. 10. The Figure implies that the refractive index increases with $h\nu$, slowly before the absorption edge, then strongly after it. Annealing increases the refractive index for all films. For $h\nu \leq 2.3$ eV, the refractive index of all the as-deposited films lies in the range 1.33–3.29, and of all annealed films in the range 1.51–4.64. The increase of the refractive index with annealing is an indication of the improvement of the crystallinity

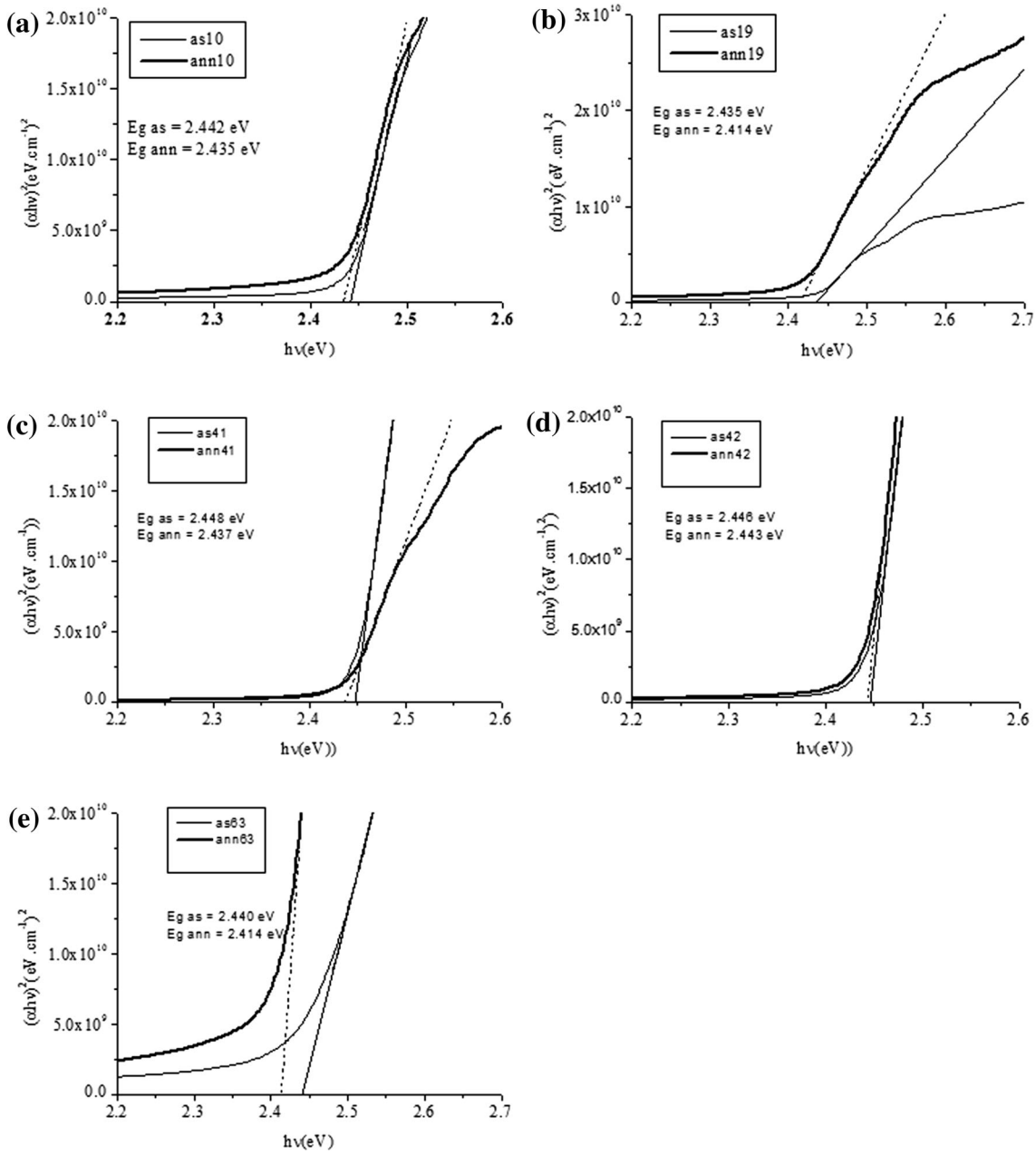

Fig. 6. The plot and linear fit of $(\alpha h\nu)^2$ against the photon's energy $h\nu$ for CdS:In films of different thickness before and after annealing. (a) t = 336 nm. (b) t = 401 nm. (c) t = 732 nm. (d) t = 741 nm. (e) t = 801 nm.

of the films. The values of n before and after annealing at wavelength λ = 550 nm for all films are inserted in Table I.

Below the absorption edge, refractive index dispersion can be analyzed by the single oscillator model. The dispersion of incident photon energy plays the important role in determining the optical property of the material. Thus, the obtained data of refractive index n has also been analyzed to yield the long wavelength refractive index (n_∞) together with the average oscillator wavelength (λ_0) for CdS:In thin film before and after annealing using the following relationship.[15]

$$\frac{n_\infty^2 - 1}{n^2 - 1} = 1 - \left(\frac{\lambda_0}{\lambda}\right)^2 \tag{4}$$

The relationship between $(n^2 - 1)^{-1}$ and λ^{-2} for the as-deposited and annealed films is shown in Fig. 11. which also shows the linear fits in the linear part of each curve, where λ_0, n_∞ and $\varepsilon_\infty = n_\infty^2$ are evaluated from the fit parameters and are listed in Table II. From these values, the average excitation energy for electronic transitions $E_0 = hc/\lambda_0$, and the dispersion energy which is a measure of the strength of inter-band optical transitions $E_d = E_0(n_\infty^2 - 1)$ are also

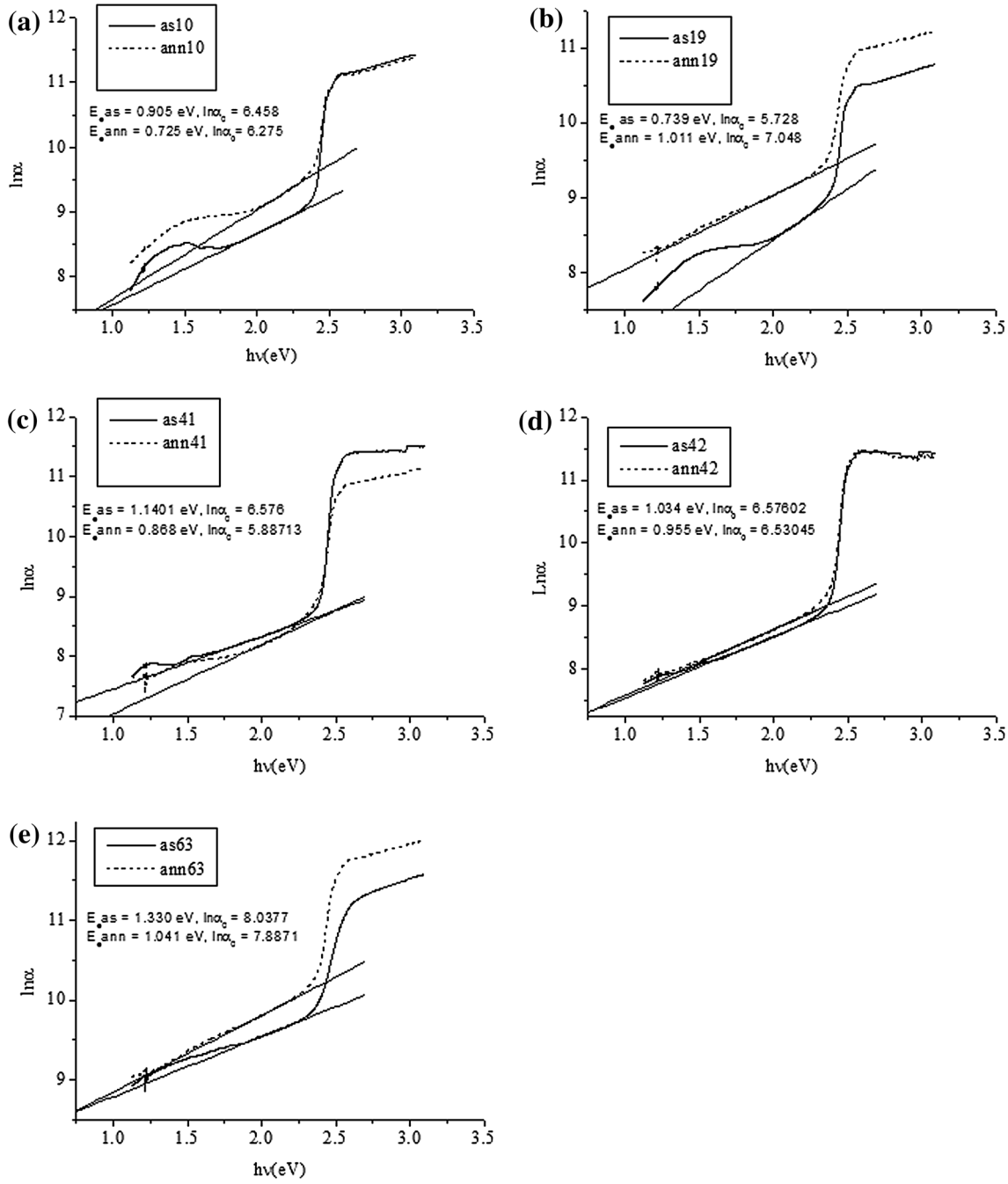

Fig. 7. A plot and linear fits of ln (α) against the photon's energy $h\nu$ for CdS:In films of different thickness before and after annealing. (a) t = 336 nm. (b) t = 401 nm. (c) t = 732 nm. (d) t = 741 nm. (e) t = 801 nm.

calculated and also listed in Table II. In general, λ_0, n_∞, ε_∞ and E_d increased with annealing, while E_0 decreased. The ratio of E_0 to E_g was calculated and is shown in Table II where i It is found that (E_0/E_g) $\approx$ 1.1. This ratio is close to 1.2, at which Ilican et al.[16] reported that the oscillator energy E_o is related to lowest direct bandgap empirically by $E_o = 1.2E_g$. So, the calculated values of E_o satisfy the empirical relationship obtained approximately from the single oscillator model. A measure of interband transition strengths can be provided from the M_{-1} and M_{-3} moments of the optical spectrum. The M_{-1} and M_{-3} are expressed as[13]

$$M_{-1} = E_d/E_0 \tag{5}$$

and

$$M_{-3} = \frac{E_d}{E_0^3}, \tag{6}$$

Table I. The optical bandgap energy E_g, width of Urbach tail E_e, α_0, and the refractive index n at λ = 550 nm for all films before and after annealing; the film thickness is also listed

Sample name	t (nm)	E_g (eV)	E_e (eV)	ln(α_0)	α_0	n (at 550 nm)
63F	336	As = 2.440	As = 1.330,	As = 8.038	As = 3095.5	3.145
		Ann = 2.414	Ann = 1.041	Ann = 7.887	Ann = 2662.7	4.306
10F	401	As 2.442	As = 0.905	As = 6.458	As = 637.8	2.082
		Ann = 2.435	Ann = 0.725	Ann = 6.275	Ann = 531.1	2.746
19F	732	As = 2.435	As = 0.739	As = 5.728	As = 307.4	2.746
		Ann = 2.414	Ann = 1.011	Ann = 7.048	Ann = 1150.6	4.308
41F	741	As = 2.448	As = 1.1401	As = 6.576	As = 717.7	2.412
		Ann = 2.437	Ann = 0.868	Ann = 5.887	Ann = 360.4	2.383
42F	801	As = 2.446	As = 1.034	As = 6.576	As = 717.8	2.952
		Ann = 2.443	Ann = 0.955	Ann = 6.530	Ann = 685.7	3.338

As As-deposited film, *Ann* annealed film.

The calculated values are shown in Table II, from which it can be observed that both moments had increased with annealing.

The polarizability of any solid is proportional to its dielectric constant. The variation of the dielectric constant with the photon's energy is an indication of interactions between photons and electrons in the films in this energy range. The real and imaginary parts of the complex dielectric constant are expressed as:[13,17]

$$\varepsilon_1 = n^2 - k^2 \tag{7}$$

and

$$\varepsilon_2 = 2nk \tag{8}$$

Figure 12 displays the relationship between ε_1 and the photon's energy $h\nu$ for all films before and after heat treatment. As seen in the Figure, ε_1 is constant or slowly increases with $h\nu$ in the near-infrared and visible regions before the absorption edge, after which an abrupt increase occurs. The variation of ε_1 is restricted in the ranges 2.28–10.83 and 2.28–21.56 for h$\nu \leq$ 2.30 eV for the as-deposited and annealed films, respectively. This abrupt increase indicates that the interaction of photons and electrons is the strongest at the absorption edge. In general, the real part of the dielectric constant increased with annealing.

Figure 13 depicts the relationship between the imaginary part of the dielectric constant ε_2 against $h\nu$ for the whole set of films before and after annealing. The behavior of ε_2 follows the behavior of k since it represents the absorption associated with free carriers.[10] The values of ε_2 before the absorption edge are constant (approximately equal to zero) before and after annealing. An abrupt increase in ε_2 occurs at the absorption edge before and after heat treatment, and the shift of the absorption edge towards longer wavelengths after heat treatment is obvious. Also, the abrupt increase in ε_2 refers to the fact that the interaction between photons and electrons is the strongest at this point.

Dielectric loss is a loss of energy that goes into heating a dielectric material in a varying electric field. The dielectric loss is given by the relationship;[15]

$$\tan\delta = \frac{\varepsilon_2}{\varepsilon_1}, \quad \text{and the loss angle is} \quad \delta = \tan^{-1}\left(\frac{\varepsilon_2}{\varepsilon_1}\right) \tag{9}$$

Figure 14 depicts the relationship between the dielectric loss and photon's energy $h\nu$ for the whole set of films before and after heat treatment. From the figure, it can be observed that the dielectric loss for some films have more than one maximum before and/or after annealing, and sharply decrease with the photon's energy after the fundamental absorption edge.

The optical conductivity σ of the CdS:In thin films can be determined using the formula;[18]

$$\sigma = \frac{\alpha n c}{4\pi} \tag{11}$$

where $c$is the speed of light. Figure 15 shows variations in the optical conductivity as a function of the photon's energy $h\nu$. The enhanced optical conductivity at the high energy side is due to the high absorbance of the films in that region. As the figure shows, the influence of annealing is not the same for all samples; σ of samples in (b and e) increased with annealing, that of samples in (a and c) decreased, and σ of the sample in (d) remained approximately unchanged. The oscillations in the high energy side are related to glass which absorbs ultraviolet light. These results can be explained in terms of the Cd:S and In: Cd ratios in the films. The film in (b) has Cd:S equal to 1.01 and its indium content is 2.10 at.%, as mentioned before. The optical conductivity of this film had considerably increased after annealing, as shown

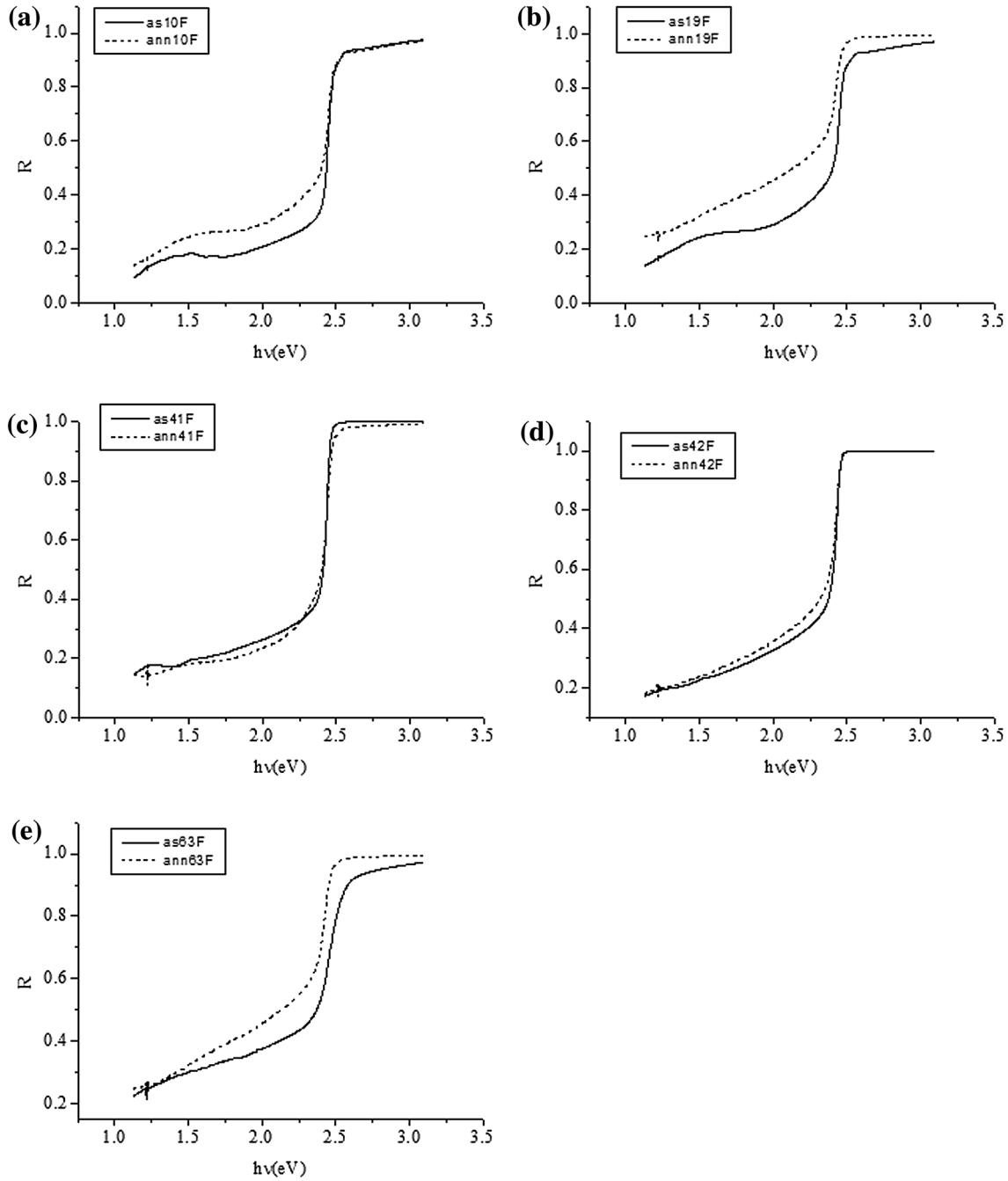

Fig. 8. The reflectivity R of CdS:In thin films of different thickness against the photon's energy $h\nu$ before and after annealing. (a) t = 336 nm. (b) t = 401 nm. (c) t = 732 nm. (d) t = 741 nm. (e) t = 801 nm.

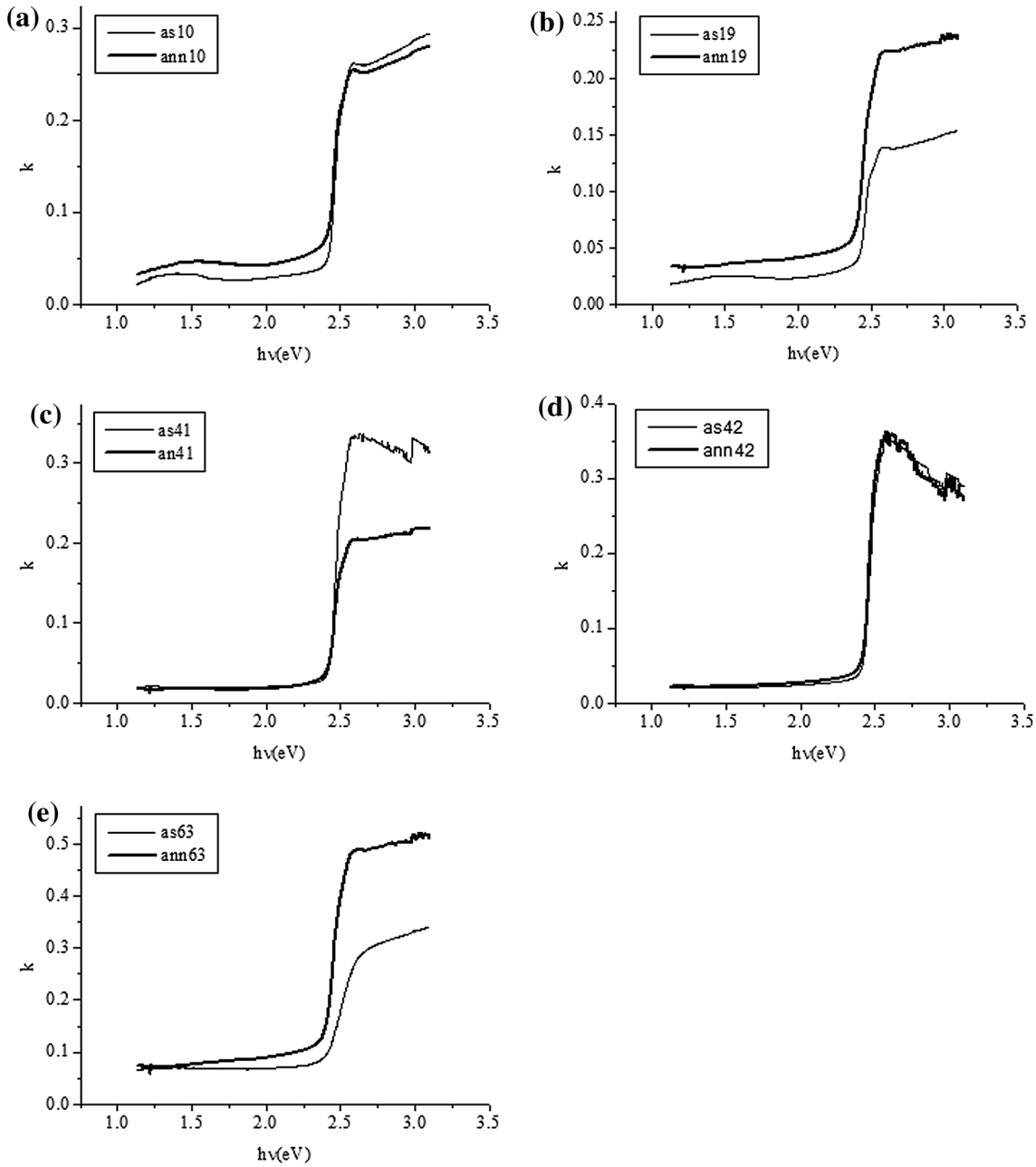

Fig. 9. A plot of the extinction coefficient k against the photon's energy $h\nu$ for CdS:In films of different thickness before and after annealing. (a) t = 336 nm. (b) t = 401 nm. (c) t = 732 nm. (d) t = 741 nm. (e) t = 801 nm.

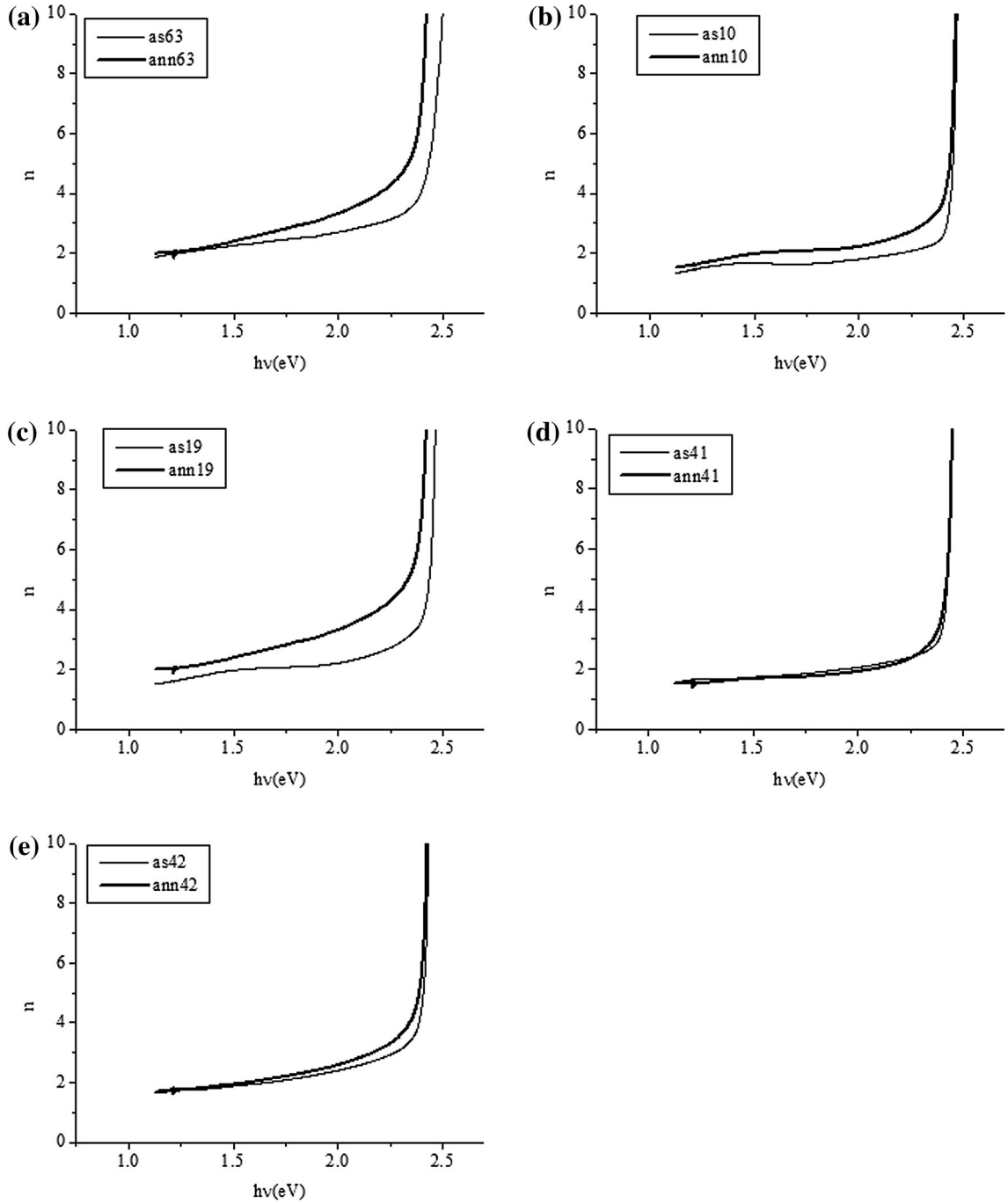

Fig. 10. A plot of the refractive index n against the photon's energy $h\nu$ for CdS:In films of different thickness before and after annealing. (a) t = 336 nm. (b) t = 401 nm. (c) t = 732 nm. (d) t = 741 nm. (e) t = 801 nm.

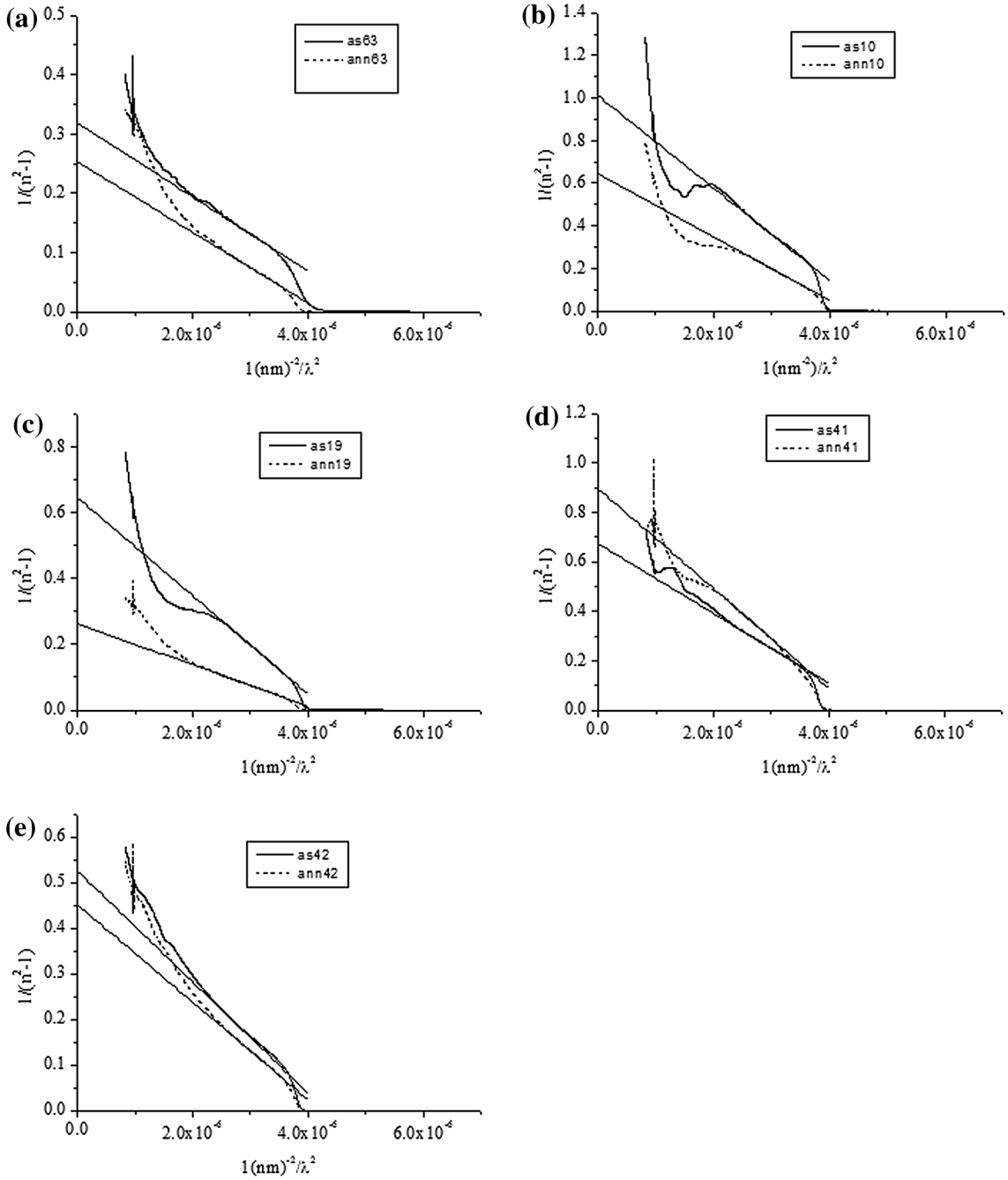

Fig. 11. The plot and linear fits of $(n^2 - 1)^{-1}$ against λ^{-2} for as-deposited and annealed CdS:In thin films of different thickness. (a) t = 336 nm. (b) t = 401 nm. (c) t = 732 nm. (d) t = 741 nm. (e) t = 801 nm.

Table II. The oscillator parameters of CdS:In thin films of different thickness before and after annealing

Sample	t (nm)	λ_0 (nm)	n_∞	ε_∞	E_0 (eV)	E_d (eV)	E_0/E_g	M_{-1} $(eV)^{-2}$	M_{-3} $(eV)^{-2}$
63F	336	442.6	2.03	4.14	2.802	8.798	As = 1.15	3.136	0.399
		485.1	2.22	4.94	2.556	10.080	Ann = 1.06	3.944	0.604
10F	401	463.6	1.410	1.988	2.675	2.642	As = 1.10	0.988	0.138
		480.8	1.596	2.548	2.579	3.992	Ann = 1.06	1.548	0.233
19F	732	480.7	1.597	2.551	2.580	4.002	As = 1.06	1.551	0.233
		489.2	2.190	4.798	2.535	9.626	Ann = 1.05	3.798	0.591
41F	741	457.5	1.577	2.488	2.710	4.032	As = 1.11	1.488	0.203
		474.8	1.455	2.118	2.612	2.919	Ann = 1.07	1.118	0.164
42F	801	481.7	1.704	2.903	2.574	4.899	As = 1.05	1.903	0.287
		486.9	1.794	3.217	2.547	5.646	Ann = 1.04	2.217	0.342

As As-deposited film, *Ann* annealed film.

in Fig. 15b. It is expected that the same situation applies for the film in €, while the other films may have Cd:S ratio less than 1.0 and they may contain less indium. This is expected for films prepared by the SP technique because it has a dynamic nature.

CONCLUSION

Polycrystalline indium-doped cadmium sulfide thin films were prepared by the SP technique on glass substrates, and the influence of heat treatment in a nitrogen atmosphere on the optical parameters of the films was studied. In general, it has been found that the transmittance and optical bandgap energy decrease with annealing, which is related to the improvement of the crystallinity of the films after annealing. On the other hand, the absorption coefficient, Urbach tail width, extinction coefficient, refractive index, and real part of the dielectric constant, increased with annealing, while the imaginary part of the dielectric constant showed small changes. The dielectric loss and optical conductivity increased for some films and decreased for others, which was explained in terms of Cd:S ratios in the films and their indium contents. These results are important for the use of CdS:In films in optoelectronic devices and thin film solar cells.

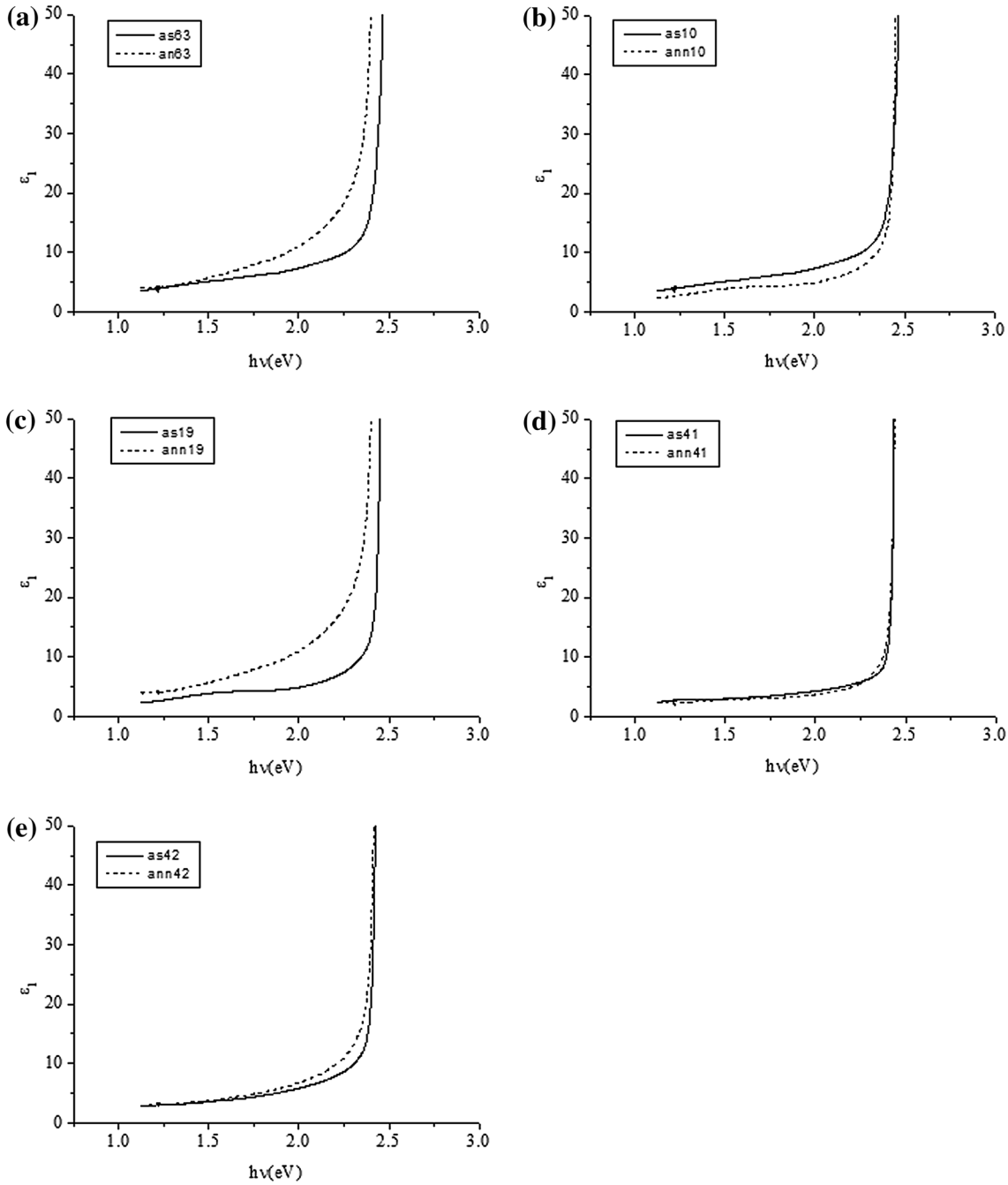

Fig. 12. The plot of the real part of the dielectric constant ε_1 against the photon's energy $h\nu$ for CdS:In films of different thickness before and after annealing. (a) t = 336 nm. (b) t = 401 nm. (c) t = 732 nm. (d) t = 741 nm. (e) t = 801 nm.

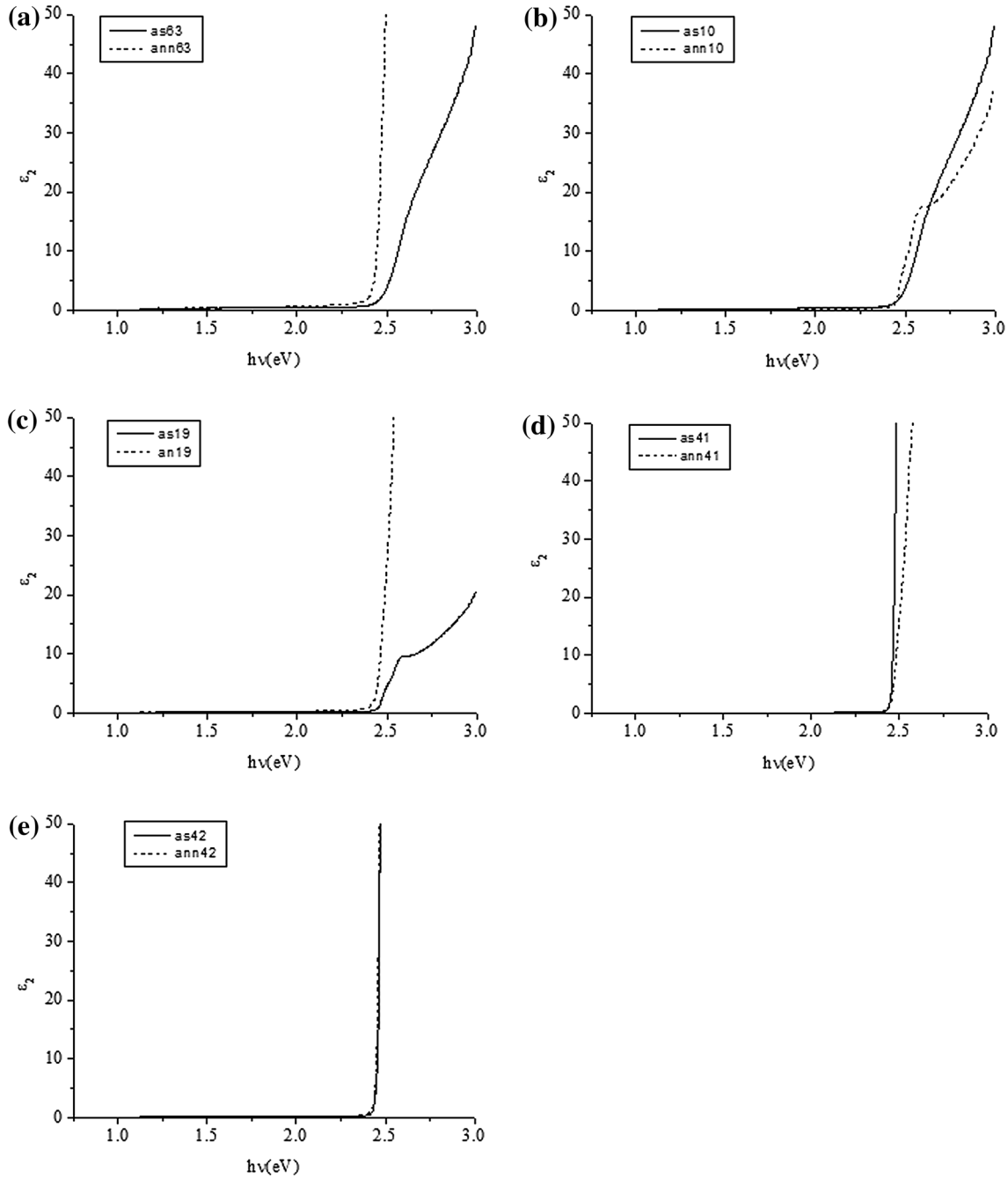

Fig. 13. The plot of the imaginary part of the dielectric constant ε_2 against the photon's energy $h\nu$ for CdS:In films of different thickness before and after annealing. (a) t = 336 nm. (b) t = 401 nm. (c) t = 732 nm. (d) t = 741 nm. (e) t = 801 nm.

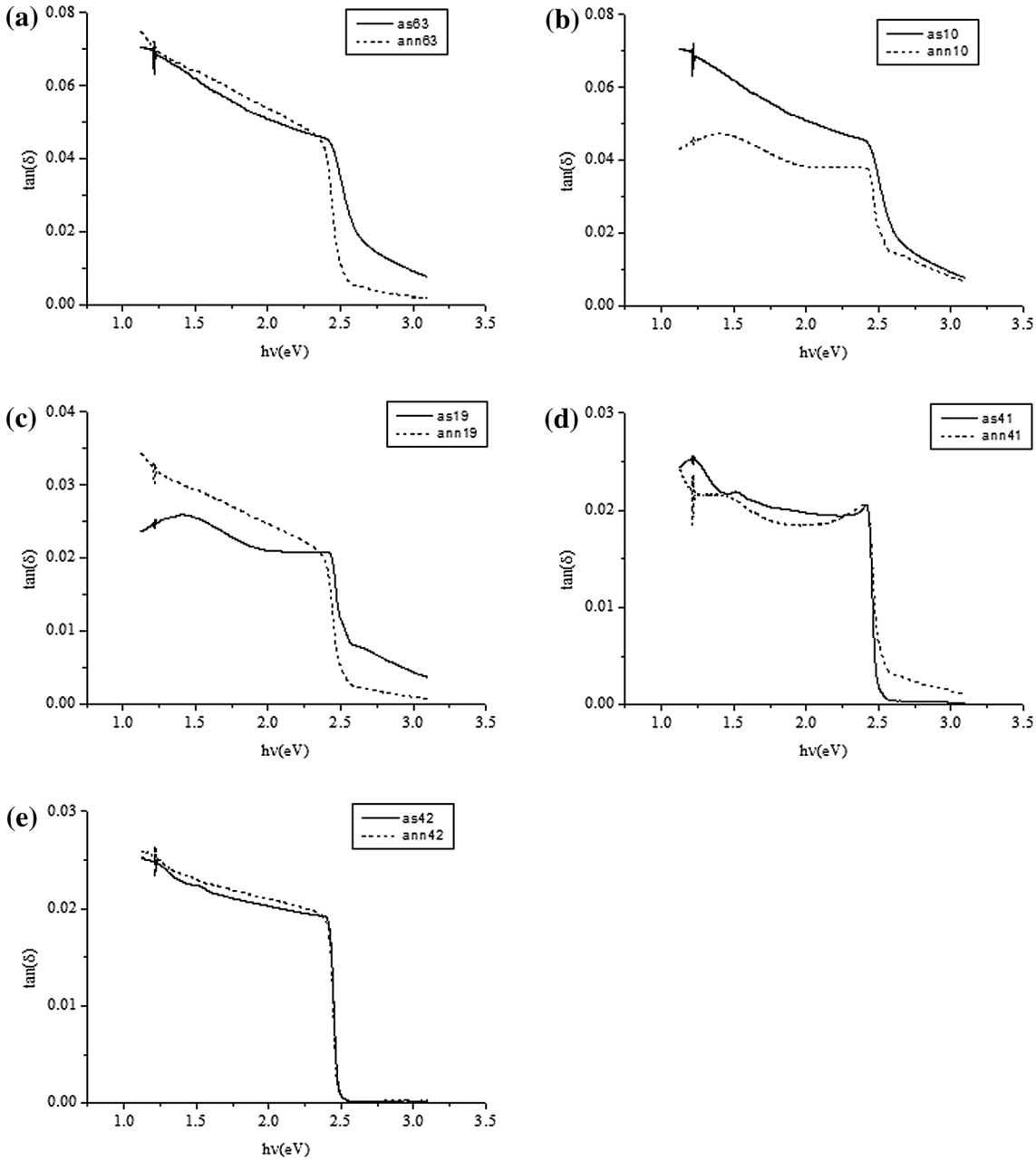

Fig. 14. The plot of the energy loss against the photon's energy $h\nu$ for CdS:In films of different thickness before and after annealing. (a) t = 336 nm. (b) t = 401 nm. (c) t = 732 nm. (d) t = 741 nm. (e) t = 801 nm.

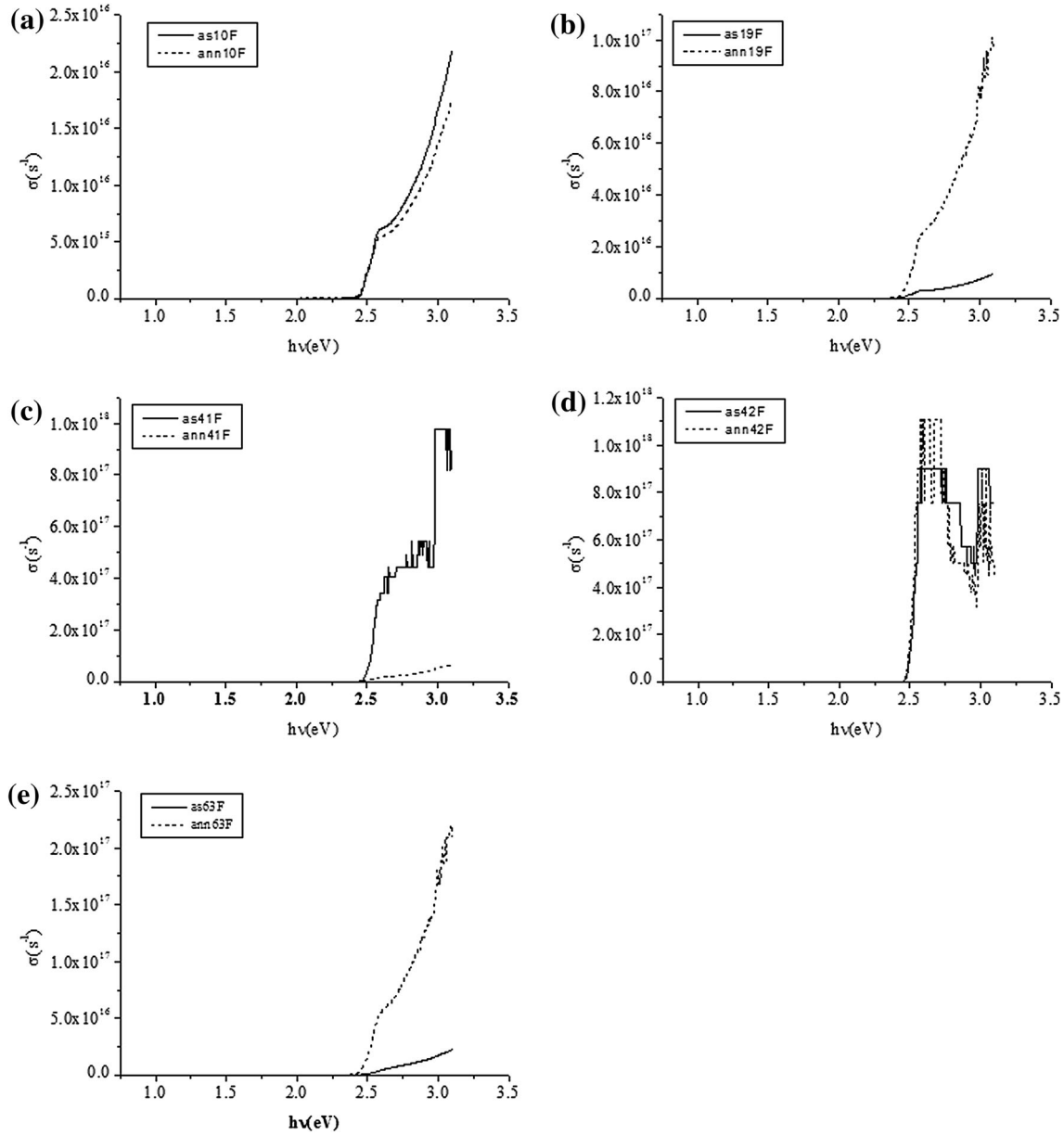

Fig. 15. The plot of the optical conductivity σ against the photon's energy $h\nu$ for CdS:In films of different thickness before and after annealing. (a) t = 336 nm. (b) t = 401 nm. (c) t = 732 nm. (d) t = 741 nm. (e) t = 801 nm.

REFERENCES

1. B. Ghosh, K. Kumar, B.K. Singh, P. Banerjee, and S. Das, *Appl. Surf. Sci.* 320, 309 (2014).
2. N.M. Megahid, M.M. Wakkad, E.K.H. Shokr, and N.M. Abass, *Phys. B* 353, 150 (2004).
3. T.D. Dzhafarov, F. Ongul, and S.A. Yuksel, *Vacuum* 84, 310 (2010).
4. G. Perna, V. Capozzi, M. Ambrico, V. Augelli, T. Ligonzo, A. Minafra, L. Schiavulli, and M. Pallara, *Thin Solid Films* 453–454, 187 (2004).
5. C.D. Lokhande and S.H. Pawar, *Solid State Commun.* 44, 1137 (1982).
6. A. Fatehmulla, A.S. Al-Shammari, A.M. Al-Dhafiri, W.A. Farooq, and F. Yakuphanoglu, *World Appl. Sci. J.* 31, 2073 (2014).
7. G. Sasikala, P. Thilakan, and C. Subramanian, *Sol. Energy Mater. Sol. C* 62, 275 (2000).
8. P.K. Nair, M.T.S. Nair, and J. Campos, *Sol. Energy Mater* 15, 441 (1987).
9. D. Fernando, M. Khan, and Y. Vasquez, *Mater. Sci. Semicond. Process.* 30, 174 (2015).
10. P.P. Sahay, R.K. Nath, and S. Tewari, *Cryst. Res. Technol.* 42, 275 (2007).
11. S.J. Ikhmayies and R.N. Ahmad-Bitar, *Am. J. Appl. Sci.* 5, 1141 (2008).
12. S.J. Ikhmayies and R.N. Ahmad-Bitar, *Appl. Surf. Sci.* 256, 3541 (2010).
13. A.A. Ziabari and F.E. Ghodsi, *Sol. Energy Mater. Sol. C* 105, 249 (2012).
14. S.S. Babkair, N.M. Al-Twarqi, and A.A. Ansari, *Karachi Univ. J. Sci.* 39, 1 (2011).

15. E.Ş. Tüzemen, S. Eker, H. Kavak, and R. Esen, *Appl. Surf. Sci.* 255, 6195 (2009).
16. S. Ilican, Y. Caglar, and M. Caglar, *Phys. Maced.* 56, 43 (2006).
17. A.A. Alnajjar, F.Y. Al-Shaikley, and M.F.A. Alias, *J. Electron Devices* 16, 1306 (2012).
18. R.L. Mishra, S.K. Mishra, and S.G. Prakash, *J. Ovonic Res.* 5, 77 (2009).